

This article was downloaded by: [University Of Gujrat]

On: 11 December 2014, At: 13:52

Publisher: Taylor & Francis

Informa Ltd Registered in England and Wales Registered Number: 1072954 Registered office: Mortimer House, 37-41 Mortimer Street, London W1T 3JH, UK



Molecular Crystals and Liquid Crystals

Publication details, including instructions for authors and subscription information:

<http://www.tandfonline.com/loi/gmcl20>

Comparative Studies on Drug Delivery Behavior of Mesoporous Silicas

Yuin Jeong^a, Sung Soo Park^a, A Reum Sung^a & Chang-Sik Ha^a

^a Department of Polymer Science and Engineering, Pusan National University, Busan, Korea

Published online: 17 Nov 2014.

To cite this article: Yuin Jeong, Sung Soo Park, A Reum Sung & Chang-Sik Ha (2014) Comparative Studies on Drug Delivery Behavior of Mesoporous Silicas, Molecular Crystals and Liquid Crystals, 600:1, 70-80, DOI: [10.1080/15421406.2014.936781](https://doi.org/10.1080/15421406.2014.936781)

To link to this article: <http://dx.doi.org/10.1080/15421406.2014.936781>

PLEASE SCROLL DOWN FOR ARTICLE

Taylor & Francis makes every effort to ensure the accuracy of all the information (the "Content") contained in the publications on our platform. However, Taylor & Francis, our agents, and our licensors make no representations or warranties whatsoever as to the accuracy, completeness, or suitability for any purpose of the Content. Any opinions and views expressed in this publication are the opinions and views of the authors, and are not the views of or endorsed by Taylor & Francis. The accuracy of the Content should not be relied upon and should be independently verified with primary sources of information. Taylor and Francis shall not be liable for any losses, actions, claims, proceedings, demands, costs, expenses, damages, and other liabilities whatsoever or howsoever caused arising directly or indirectly in connection with, in relation to or arising out of the use of the Content.

This article may be used for research, teaching, and private study purposes. Any substantial or systematic reproduction, redistribution, reselling, loan, sub-licensing, systematic supply, or distribution in any form to anyone is expressly forbidden. Terms & Conditions of access and use can be found at <http://www.tandfonline.com/page/terms-and-conditions>

Comparative Studies on Drug Delivery Behavior of Mesoporous Silicas

YUIN JEONG, SUNG SOO PARK, A REUM SUNG,
AND CHANG-SIK HA*

Department of Polymer Science and Engineering, Pusan National University,
Busan, Korea

In this work, we compared drug delivery behaviors of two different mesoporous materials, SBA-15 and MCM-41. For this work, mesoporous materials were modified with alkylsilane-containing secondary dialkylammonium ions (SAPH) and macrocyclic materials (DB24C8). The mesostructure and modified surface of mesoporous materials were characterized by multi-techniques. We used ibuprofen, lysozyme, and cytochrome c as the drug molecules. The photoluminescent spectra of releasing drug molecules from mesoporous materials showed controlled releasing behavior on adding base solutions. We found that the drug release behavior was strongly dependent on the pore size of the materials and the size of the drug molecules.

Keywords SBA-15; MCM-41; modified mesoporous materials; drug molecule; enzyme; controlled release

Introduction

Even though many reports on the synthesis of MCM and SBA families having various mesostructures are reported in the literature [1, 2], the development of MCM-41 and SBA-15 have led to great interest in the material sciences, owing to their easy fabrication method and well-defined mesostructures. More diverse applications of the two mesoporous materials remain a challenging endeavor facing today's chemists.

On the other hand, the controlled release of drug molecules from an inert matrix has become increasingly important for a variety of biomedical systems due to the advantages of safety, efficiency, and patient convenience. Many works have been done on the drug adsorption and release properties of mesoporous silica materials [3–5].

The ibuprofen, an anti-inflammatory drug, was selected as a model drug due to its low solubility in water and its small molecular size ($1.0 \times 0.6 \text{ nm}^2$); therefore, it is suitable for incorporation within the mesopores [6]. Meanwhile protein hen egg white lysozyme has received particular attention because of its well-understood structural characteristics [7]. Lysozyme is widely distributed in various biological fluids and tissues, including avian egg, plant and animal secretions [8]. The isoelectric point (pI) of lysozyme is around 11.

*Address correspondence to Chang-Sik Ha, Department of Polymer Science and Engineering, Pusan National University, Busan 609-735, Korea. Tel.: +82-51-510-2407; Fax: +82-51-514-4331. E-mail: csha@pnu.edu

Color versions of one or more of the figures in the article can be found online at www.tandfonline.com/gmcl.

In addition, cytochrome c has often been studied in immobilization studies [9], with many of the factors governing its immobilization known with an isoelectric point of 9.8 [10].

In this work, we have compared the drug delivery behavior of SBA-15 and MCM-41. Although some scattered literatures report drug delivery behavior of SBA-15 and MCM-41 independently, no reports have been published on the direct comparison of the two mesoporous materials. For this work, alkylsilane-containing secondary dialkylammonium ions and macrocyclic materials are used for the modification of the mesoporous materials. We used ibuprofen, lysozyme, and cytochrome c as the drug molecules for comparison.

Experimental

Materials

Hen egg white lysozyme, horse heart cytochrome c, ibuprofen, toluene (C_7H_8), and dibenzo [24] crown-8 (DB24C8) were obtained from Sigma Aldrich and used without further purification. SBA-15 and MCM-41 with different pore diameters were synthesized with tetraethyl orthosilicate (TEOS), Pluronic P123 ($EO_{20}PO_{70}EO_{20}$: EPE, $M_n = 5800$), and cetyltrimethylammonium bromide (CTABr), according to a literature procedure [1, 2]. All reagents were purchased from Sigma Aldrich and used as received. Hydrochloric acid (HCl) and sodium hydroxide (NaOH) were purchased from Junsei and 3-(N-styrylmethyl-2-aminoethylamino) propyltrimethoxysilane hydrochloride (SAPH) was purchased from Gelest. They were also used as received.

MCM-41 has been hydrothermally synthesized in sodium hydroxide medium with low surfactant concentration according to the reported procedure [1]. In addition, SBA-15 was also synthesized as conventional methods using triblock copolymer, Pluronic P123, as the templating agent and TEOS as the silica source in an acidic medium [2]. We used as-synthesized samples to modify SBA-15 without further solvent extraction or calcination. The surfactant-removed MCM-41 and as-synthesized SBA-15 were modified with SAPH. To remove water which is bonded with surface silanol groups, MCM-41 was degassed at 300°C over 5 h under vacuum condition. In the case of SBA-15, to protect surfactant of as-synthesized SBA-15, the sample was dried at 80°C for 3 h in drying oven. The 0.5 g of degassed or dried sample was dissolved in 0.1 M SAPH in toluene and stirred at room temperature for 12 h. The products were filtered and washed with toluene several times and then they were dried at 80°C . The modified SBA-15 was dissolved in ethanolic HCl (150 ml of EtOH and 3 ml of HCl per 1 g of sample) to remove remaining surfactant from inner wall surface of the modified SBA-15. These hybrid materials were loaded subsequently with 0.15 mol/L of ibuprofen in hexane, or 75 $\mu\text{mol/L}$ of lysozyme or cytochrome c in buffer solution (pH 9.6 sodium bicarbonate buffer), and the pores were further modified with DB24C8 of 10 mM in acetic acid.

Measurements and Characterization

X-ray diffraction (XRD) patterns were recorded on a Rigaku D/MAX-III diffractometer using the x-ray radiation source of $\text{CuK}\alpha$ radiation ($\lambda = 1.5406\text{\AA}$). Small angle X-ray scattering (SAXS) was performed at Pohang Accelerator Laboratory (PAL), Korea with $\text{CoK}\alpha$ ($\lambda = 1.608\text{\AA}$) radiation. Nitrogen adsorption and desorption isotherms were measured at 77 K using a Nova 4000e surface Area & pore size analyzer. Prior to measurement samples were dehydrated in vacuum. Samples with KBr pellets were characterized by FT-IR spectroscopy at ambient atmosphere. All the spectra were recorded averaging 24

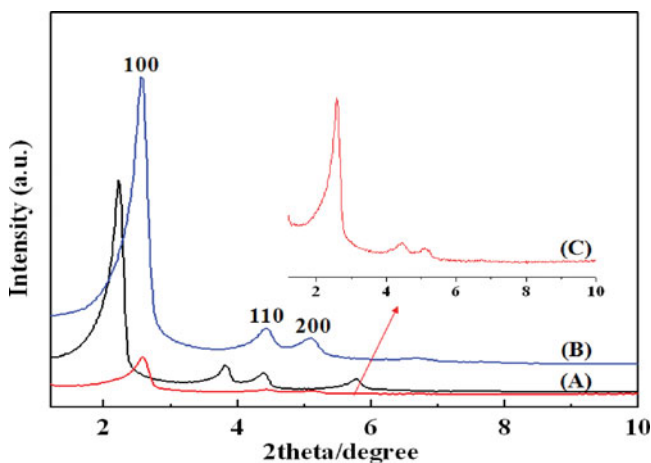


Figure 1. X-ray diffraction (XRD) patterns of MCM-41: (A) as-synthesized, (B) calcined, and (C) modified MCM-41.

scans at 16 mm^{-1} resolution on a Shimadzu IR Prestige-21 spm using a Ge-KBr beam splitter. The photoluminescence spectra were measured with HITACHI Instrument F-4500 Fluorescence spectrophotometer equipped with a xenon lamp. The excitation wavelength was 303 nm, 346 nm, 375 nm and 430 nm and the wavelength from 200 nm to 800 nm range was scanned.

Results and Discussion

The XRD patterns of calcined MCM-41 and modified MCM-41 as well as the as-synthesized MCM-41 are shown in Fig. 1. All patterns exhibit four sharp Bragg peaks, which can be indexed as 100, 110, 200 and 210 reflections of $p6mm$ hexagonal symmetry. The calcined MCM-41 sample has lattice d-spacing of 3.4, 2.0, 1.7, and 1.3 nm, respectively. Using the obtained d_{100} value, the pore diameter is finally determined as 2.9 nm. Fig. 1 shows that the hexagonal mesostructure of MCM-41 was well retained even after modification for the modified MCM-41.

SAXS patterns of samples are shown in Fig. 2. All the SAXS patterns exhibit well-resolved peaks (prominent peaks at $0.06, 0.11, 0.12 \text{ \AA}^{-1}$) that can be indexed as the 100, 110, and 200 reflections of $p6mm$ hexagonal symmetry with lattice d-spacing of 10.5, 5.7, and 5.2 nm, respectively. The corresponding unit cell parameter, a_0 , is 12.1 nm. Comparing the SAXS patterns clearly shows that the modification of SAPH does not affect the SBA-15 mesostructure. However, the slight decrease of the relative reflection intensities of 100 peaks for the modified SBA-15 indicates that the pores of the solvent-extracted SBA-15 are blocked to some degree by SAPH during the modification process. On the other hand, in the case of the solvent extracted SBA-15 after modification, SAPH are anchored to the entrance and outside wall of the as-synthesized SBA-15, resulting in the larger pore size than the modified SBA-15.

Suitable nanocontainers for drugs should have a pore size of 30 \AA or larger for the accessibility of lysozyme and cytochrome c to the internal surface of the mesopores. Therefore, it can be said that the pore size of SBA-15 is larger enough to allow accessing those enzymes. Also, the modified mesoporous silica after solvent extraction is believed to be proper to prepare nanocontainers for drug delivery.

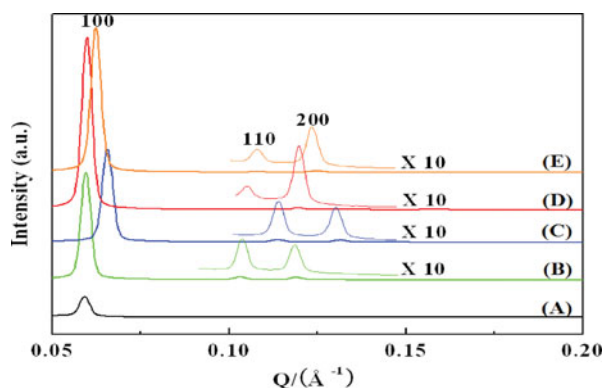


Figure 2. Small angle x-ray scattering (SAXS) patterns of (A) as-synthesized, (B) solvent extracted, (C) after modification and then solvent extracted, (D) after solvent extraction and then modified, and (E) calcined SBA-15.

Figure 3 illustrates the transmission FT-IR spectra of calcined MCM-41, modified MCM-41, as-synthesized SBA-15, solvent extracted SBA-15, before-modified SBA-15 and after-modified SBA-15 casted on a KBr crystal. After pore surface modification by SAPH (Fig. 3(A)–(B) (top), (C) and (D) (bottom)), both 2880 cm^{-1} and 2980 cm^{-1} for aliphatic

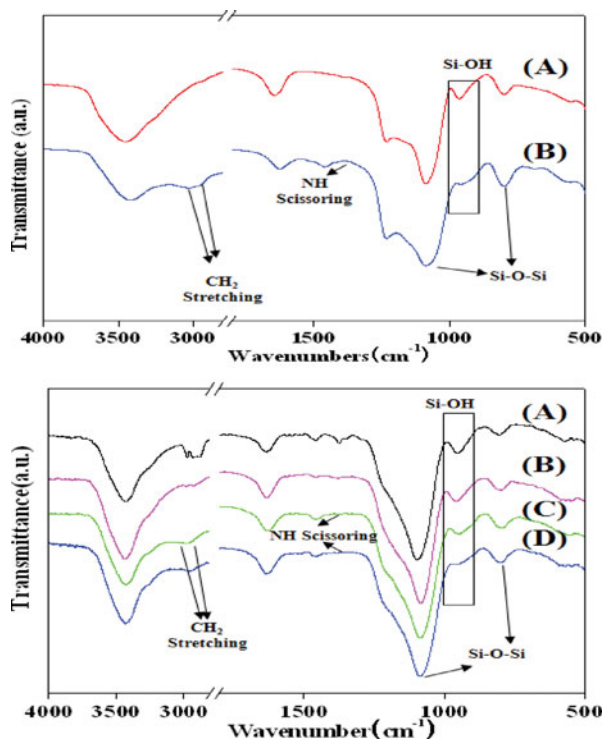


Figure 3. FT-IR spectra of MCM-41(top) and SBA-15 (bottom): (top) (A) calcined MCM-41, (B) modified MCM-41, (bottom) (A) as-synthesized SBA-15, (B) solvent extracted SBA-15, (C) after-modified SBA-15, (D) before-modified SBA-15.

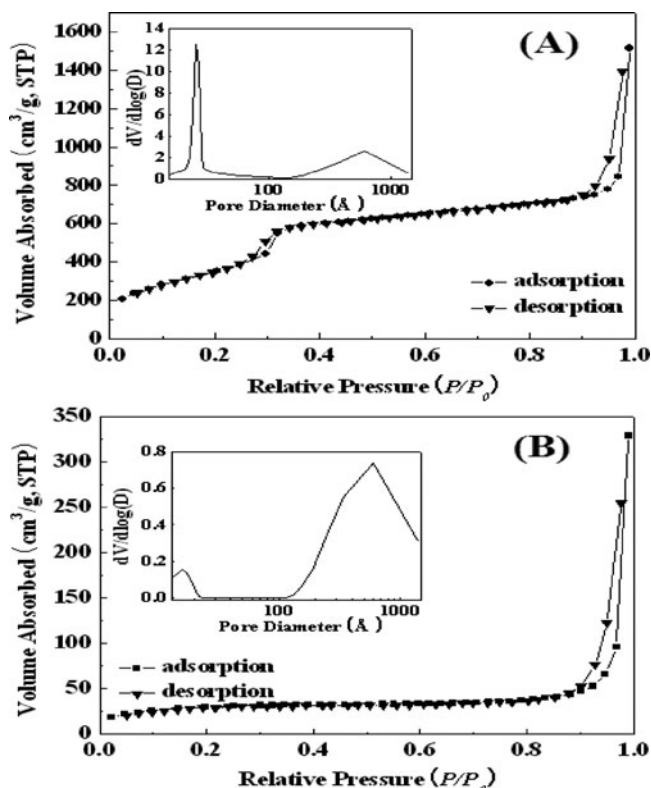


Figure 4. Nitrogen adsorption and desorption isotherms of MCM-41 (A), modified MCM-41 (B). Insert figures exhibit the pore size distribution for each sample.

CH stretching, 1538 cm^{-1} for NH scissoring, 1460 cm^{-1} for CH_2 bending can be assigned. On the other hand, the peak at 950 cm^{-1} for silanol group of modified mesoporous silicas was disappeared. This is due to the formation of Si-O-Si linkage between SAPH and mesoporous silica by sol-gel reactions. Especially, in the case of SBA-15 (Fig. 3-(bottom)), we can see the difference of the intensity of the Si-OH band. In the case of (D), we can know that almost all the Si-OH surface groups were modified with SAPH. On the other hand, in the case of (C), we see that Si-OH groups of the inside wall remain on SBA-15 through the influence of templates before solvent extraction. The results of FT-IR analysis in Fig. 3 supports that the method of modification before solvent extraction is better than the modification after solvent extraction.

The isotherms of nitrogen adsorption and desorption on mesoporous silicas and the corresponding pore size distribution curves calculated using Barrett-Joyner-Halenda (BJH) method [11] are shown in Figs. 4 and 5. Nitrogen adsorption isotherms of calcined MCM-41, solvent extracted SBA-15 and modified SBA-15 belong to type IV isotherms. The isotherms of SBA-15 series show a reversible part and type A hysteresis loop at higher pressures.

The textural characteristics of the corresponding samples are summarized in Table 1. After modification of MCM-41 (Fig. 4(B)), all the Brunauer-Emmett-Teller (BET) surface area, pore size and pore volume are markedly reduced compared with the calcined MCM-41.

Table 1. Textural parameters of calcined MCM-41, modified MCM-41, before-modified SBA-15, after-modified SBA-15, ethanolic HCl-solvent extracted SBA-15 and toluene-solvent extracted SBA-15

	S_{BET} (m^2g^{-1})	D (\AA)	V_{total} (m^3g^{-1})
Calcined MCM-41	1350	25	2.3
Modified MCM-41	105	16	0.5
Before-modified SBA-15	248	52	0.45
After-modified SBA-15	191	37	0.36
Ethanolic HCl-solvent extracted SBA-15	663	53	1.07
Toluene-solvent extracted SBA-15	653	69	0.97

S_{BET} (m^2g^{-1}): total surface area, D (\AA): pore diameter of mesopore, V_{total} (m^3g^{-1}): total pore volume

This result indicates that SAPH has been anchored to the inner wall of calcined MCM-41 so that the pores are filled and the entrances of pores are blocked with SAPH.

In Fig. 5 (A), the surface area and pore volume are decreased comparing with the solvent extracted SBA-15 under ethanol and HCl solution(Fig. 5(C)). This result can be explained through the Fig. 5(D). The Fig. 5(D) is the nitrogen adsorption-desorption isotherm of the SBA-15 which has been stirred in toluene under room temperature for 12 hours. In this

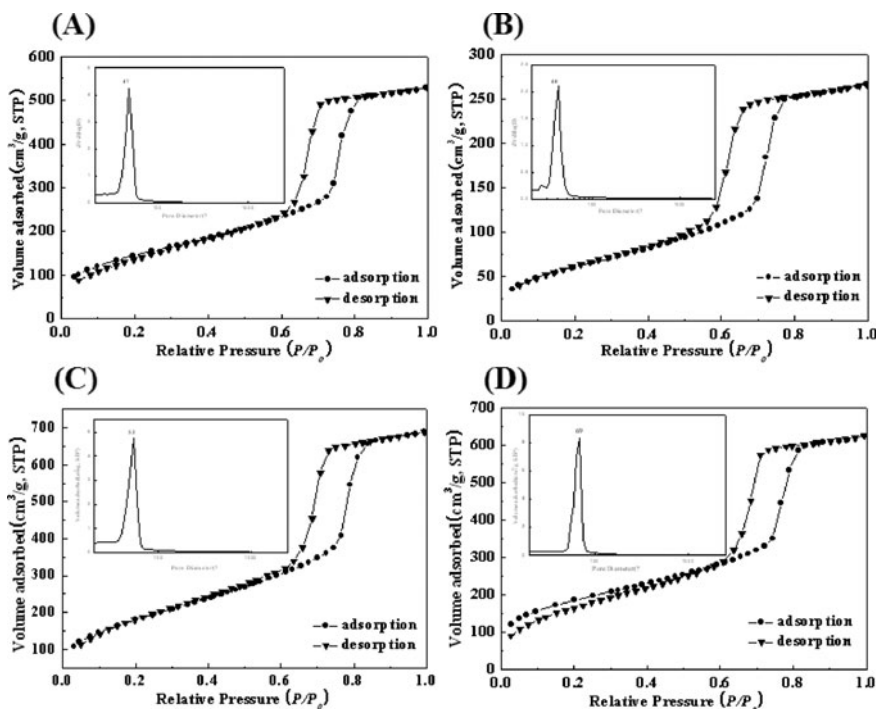
**Figure 5.** Nitrogen adsorption and desorption isotherms of (A) before-modified SBA-15, (B) after-modified SBA-15, (C) ethanolic HCl-solvent extracted SBA-15 and (D) toluene-solvent extracted SBA-15. Insert figures exhibit the pore size distribution for each sample.

Table 2. The emission maxima of buffer solutions at two different pHs (4 and 10)

λ_{ex}	303 nm	346 nm	375 nm	430 nm
pH 4	338 nm	392 nm	429 nm	503 nm
pH 10	417 nm	426 nm	429 nm	503 nm

figure, we can see that the templates are removed by organic solvent, toluene. Accordingly, when SAPH are modified to SBA-15, templates of pore entrances are removed at the same time. Also, SAPH anchored to pore entrances interrupts the permeation of hydrochloric acid in ethanol so that some templates of SBA-15 remain inside the channel.

In Fig. 5(B), for after-modified SBA-15, the pore diameter decreases from 5.3 to 3.5 nm and the surface area and pore volume also decrease comparing to those of the before-modified SBA-15 (Fig. 5(A)). This result indicates that SAPH is modified inside mesoporous wall. Therefore, the method of modification before solvent extraction is better than the modification after solvent extraction for using drug molecules of large size like lysozyme and cytochrome c.

The photoluminescence (PL) properties of the samples were characterized by emission spectra. The emission peaks of pure buffer solutions are expected from the analysis of released solutions. DB24C8 was put together to help blocking drugs in the mesoporous materials for more efficient control of drug delivery. The emission spectra of pure solutions of ibuprofen, DB24C8, lysozyme and cytochrome c are first measured. The textural emission peaks of the corresponding of drug molecules and crown ether are summarized in Table 2. The emission spectra were obtained by the excitation at 303 nm (ibuprofen), 346 nm (DB24C8), 375 nm (lysozyme) and 430 nm (cytochrome c). The emission maximum of the pH 4 and pH 10 buffer solutions used in releasing experiments are measured at 303 nm, 346 nm, 375 nm and 430 nm by excitation of ibuprofen, DB24C8, lysozyme and cytochrome c, respectively.

In Table 2 and 3, we can expect to observe emission peaks of 405 nm, 458 nm and 470 nm for released solutions included drug molecules. As shown in the Fig. 6, DB24C8 seemed to play a certain role to block the pores and to “control” the release of drugs from the mesoporous materials for both MCM-41 and SBA-15 by adding base stimuli, pH10 buffer solution, though water-insoluble DB24C8 does not completely cap the pore entrances of the mesoporous materials. These results of all samples are clearly shown from that the emission peak of DB24C8 exhibits at 419 nm.

Table 3. The emission maxima of drug molecules (ibuprofen, lysozyme, cytochrome c) and dibenzo[24]crown-8

Molecules (λ_{ex})	Emission (λ_{em})
Ibuprofen (303 nm)	405 nm
Lysozyme (375 nm)	419 nm
Cytochrome C (430 nm)	458 nm / 518 nm
DB24C8 (346 nm)	470 nm
Ibuprofen (303 nm)	405 nm

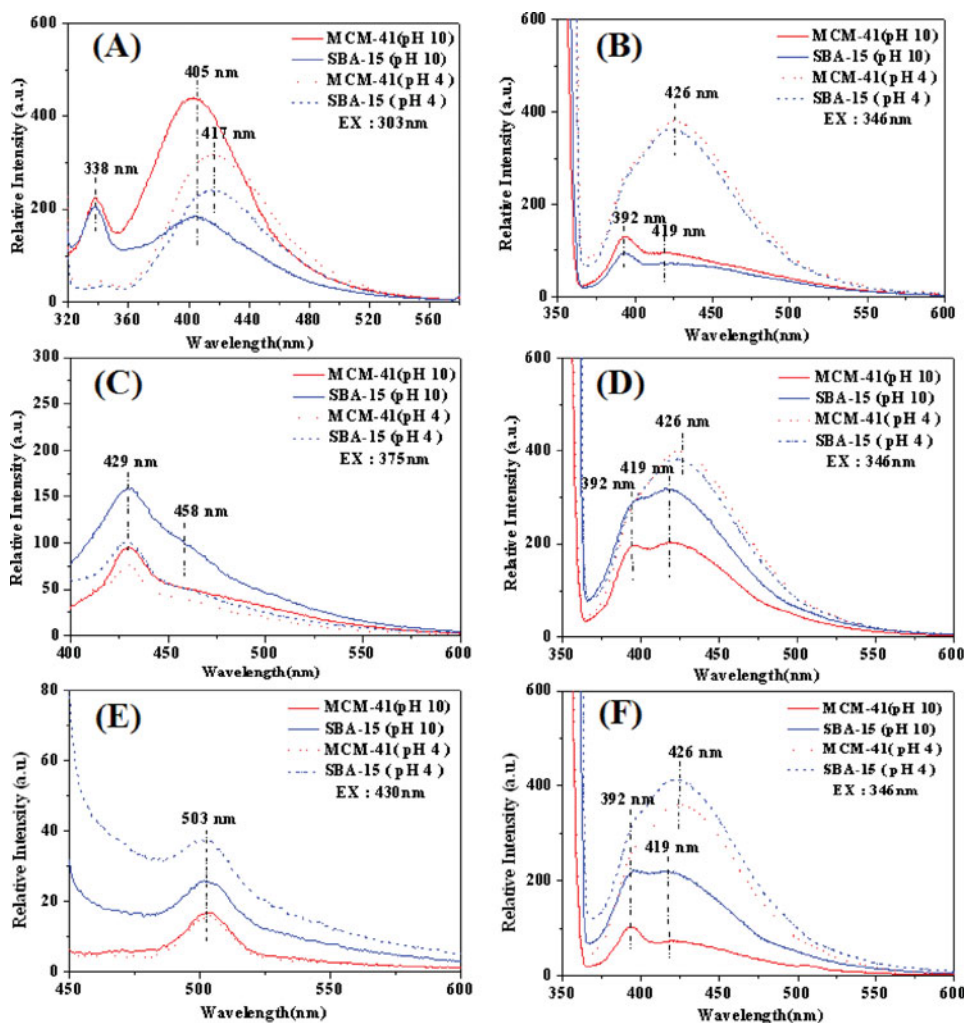


Figure 6. Photoluminescence spectra of drug-loaded MCM-41 and SBA-15 at two different excitation wavelengths. (A), (B) ibuprofen, dibenzo[24]crown-8, (C), (D) lysozyme, dibenzo[24]crown-8, and (E), (F) cytochrome c, dibenzo[24]crown-8, respectively.

DB24C8 is a sufficiently large macrocyclic polyether to be able to encircle dialkylammonium ion centers ($-\text{CH}_2\text{NH}_2^+\text{CH}_2-$), thus forming [2]-pseudorotaxanes. Since the noncovalent bonding responsible for the formation of these 1:1 complexes involves inter alia, $[\text{N}-\text{H}\cdots\text{O}]^+$ hydrogen bonds, they can be made to dissociate in solution on addition of base. The unthreaded form of [2] pseudorotaxane at the high pH values may help to release drugs from the mesoporous materials, while threading of the $-\text{CH}_2\text{NH}_2^+\text{CH}_2-$ tether SAPH with DB24C8 beads may block the release of drugs to some degree, inducing the “controlled” release behavior. Dethreading may be achieved using a range of bases [12].

In Fig. 6(B), only the emission of pH 4 buffer solution was shown under acid condition, while the emission peak of DB24C8 was shown at 419 nm under base condition. This phenomenon can be shown in Fig. 6 (D) and (F).

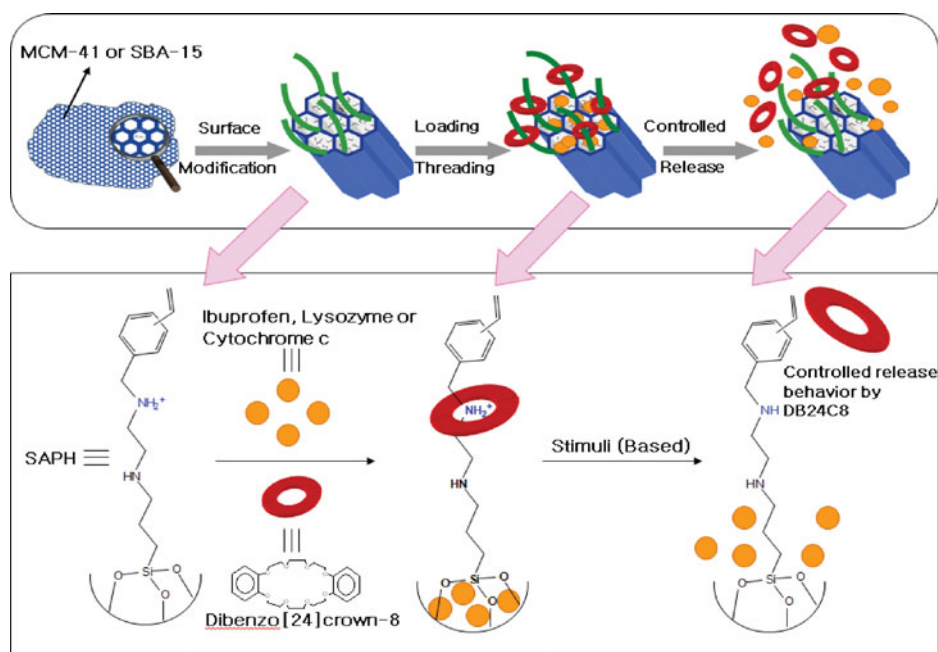


Figure 7. Schematic illustration of drug delivery behavior of mesoporous silicas.

However, the emission peaks in Fig. 6(B) show the different tendency with (D) and (F). Fig. 6(B) exhibits similar intensity in the case of MCM-41 and SBA-15 based valves, and lower intensity comparing to (D) and (F). This result indicates that ibuprofen possessing $-\text{COOH}$ group are released with DB24C8 with crown ether further complexed environment leading to the lower intensity for the emission of DB24C8 comparing to (D) and (F) [13].

As shown in Fig. 6(D) and (F), we can see that more DB24C8 are released in the case of SBA-15 than the MCM-41. These results indicate that modified SBA-15 have more SAPH, where DB24C8 is tethered, than the modified MCM-41. The releasing of drug molecules is shown in Fig. 6(A), (C) and (E).

If the emission peaks of pure buffer solution are excluded from all samples, Fig. 6(A) exhibits the releasing of ibuprofen from mesoporous materials under basic condition. The modified SBA-15 has larger pore size, pore volume and surface area than the modified MCM-41. Therefore we have expected that more ibuprofens are loaded to SBA-15. However, contrary to our expectations, the modified SBA-15 includes less ibuprofen, because ibuprofen of small sizes is leaked out from SBA-15 of large sizes.

In the case of using lysozyme as guest molecule, SBA-15 releases lysozyme, resulting in the weak shoulder of lysozyme at 458 nm. On the other hand, the MCM-41 cannot load lysozyme, which has larger size than that of pores in MCM-41, and the releasing phenomenon can not be shown.

We used cytochrome c as well as ibuprofen and lysozyme. Since cytochrome c has also large size, we have expected that the releasing phenomenon will be observed in SBA-15 only. However, contrary to our expectation, we could not observe the emission peak for all mesoporous samples. The SBA-15 before-modification is anchored to the entrance and outside walls of pores by SAPH. These SAPH chains of the entrance disturb the loading of cytochrome c to pores of SBA-15. Also lysozyme has prolate spheroid shape resulting

in the loading of lysozyme in longitudinal direction while cytochrome c possesses 3D pseudo-square type. Therefore the emission of lysozyme was observed but cytochrome c is not loaded to SBA-15. These results of emission spectra indicate that the drug delivery was operated by changing pH. Also, we know that the releasing behaviors are affected by the size of drug molecules and mesoporous silicas. Figure 7 summarizes schematically drug delivery behavior of mesoporous silicas for this work.

Conclusions

In this work, we have compared drug delivery behaviors of two different mesoporous silicas, SBA-15 and MCM-41. For this work, alkylsilane-containing secondary dialkylammonium ions (SAPH) and macrocyclic materials (DB24C8) were used for the modification of mesoporous materials and for the control of drug delivery, respectively. We used ibuprofen, lysozyme, and cytochrome c as the drug molecules for comparison. XRD and SAXS patterns showed that MCM-41 and SBA-15 have well-ordered hexagonal structure. The samples are also stable and the structures are still preserved after modification. We can also confirm the modification of SBA-15 before solvent extraction is a proper way to use for containers of drug molecules in nanovalves. It was found that the PL spectra of releasing guest molecules from the mesoporous silicas showed control releasing properties on adding base solutions. For MCM-41, the emission peaks of ibuprofen released from pores are observed. On the other hand, lysozyme ($1.9 \times 2.5 \times 4.5 \text{ nm}^3$) and cytochrome c ($2.6 \times 3.2 \times 3.3 \text{ nm}^3$) are not loaded to pores of MCM-41 due to their larger size than pore size. For SBA-15, the modified SBA-15 released less ibuprofen, because ibuprofen of small size ($1.0 \times 0.6 \text{ nm}^2$) is leaked out from SBA-15 of large size. In addition, we could see the emission of lysozyme released from the modified SBA-15 but releasing of cytochrome c was not observed. These results indicate that lysozyme of prolate spheroid shape are loaded in longitudinal direction while cytochrome c of spherical shape are not loaded to pores.

Acknowledgments

The work was done in part during CSH's overseas studies in University of California at Los Angeles (UCLA) in 2010–2011 under the subject, "Preparation and Application of Nanovalves Based on Periodic Mesoporous Organosilicas." The work was supported by the Research Institute of Industrial Technology, Pusan National University (PNU), Korea. CSH thanks to Prof. Jeffrey I. Zink of UCLA and Dr. Wanping Guo of PNU for their helpful and valuable discussions on the work.

Funding

The work was financially supported by the National Research Foundation of Korea (NRF) Grant funded by the Ministry of Science, ICT, and Future Planning, Korea (Pioneer Research Center Program (2010-0019308/2010-0019482) and Brain Korea 21 Plus Program (21A2013800002)).

References

- [1] Kresge, C., Leonowicz, M., Roth, W., Vartuli, J., & Beck, J. (1992). *Nature*, 359, 710.
- [2] Zhao, D., Huo, Q., Feng, J., Chmelka, B. F., & Stucky, G. D. (1998). *J. Am. Chem. Soc.*, 120, 6024.

- [3] Barbe, C., Bartlett, J., Kong, L. G., Finnie, K., Lin, H. Q., Larkin, M., Calleja, S., Bush, A., & Calleja, G. (2004). *Adv. Mater.*, *16*, 1959.
- [4] Regí, M. V., Balas, F., & Arcos, D. (2007). *Angew. Chem. Int. Ed.*, *46*, 7548.
- [5] Mellaerts, R., Aerts, C. A., Humbeeck, J. V., Augustijns, P., Mooter, G. V., & Martens, J. A. (2007). *Chem. Commun.*, *13*, 1375.
- [6] Izquierdo-Barba, I., Martínez, Á., Doadrio, A. L., Pérez-Pariente, Joaquin, & Vallet-Regí, M. (2005). *Europ. J. Pharmacol. Sci.*, *26*, 365.
- [7] Park, S. S., & Ha, C.-S. (2005). *Chem. Mater.*, *17*, 3519.
- [8] Jayasundera, S., Burleighm, M. C., Zeinali, M., Spector, M. S., Miller, J. B., Yan, W., Dai, S., & Markowitz, M. A. (2005). *J. Phys. Chem. B*, *109*, 9198.
- [9] Vinu, A., Murugesan, V., Tangermann, O., & Hartmann, M. (2004). *Chem. Mater.*, *16*, 3056.
- [10] Lee, C.-H., Lang, J., Yen, C.-W., Shih, P.-C., Lin, T.-S., & Mou, C.-Y. (2005). *J. Phys. Chem. B*, *109*, 12277.
- [11] Barrett, E., Joyner, L., & Halenda, P. (1951). *J. Am. Chem. Soc.*, *73*, 373.
- [12] Glink, P. T., Schiavo, C., Stoddart, J. F., & Williams, D. J. (1996). *Chem. Commun.*, 1483.
- [13] Yang, P., Ouan, Z., Li, C., Kang, X., Lian, H., & Lin, J. (2008). *Biomaterials*, *29*, 4341.